(2)

TECHNICAL REPORT BRL-TR-3275

BRL

EXPERIMENTAL MEASUREMENT OF TAILBOOM STRAIN DURING CHARGE IGNITION

JOSEPH W. COLBURN
ARTHUR A. KOSZORU

OCTOBER 1991

U.S. ARMY LABORATORY COMMAND

BALLISTIC RESEARCH LABORATORY
ABERDEEN PROVING GROUND, MARYLAND

NOTICES

Destroy this report when it is no longer needed. DO NOT return it to the originator.

Additional copies of this report may be obtained from the National Technical Information Service, U.S. Department of Commerce, 5285 Port Royal Road, Springfield, VA 22161.

The findings of this report are not to be construed as an official Department of the Army position, unless so designated by other authorized documents.

The use of trade names or manufacturers' names in this report does not constitute indorsement of any commercial product.

REPORT DOCUMENT PAGE

Form Approved
OMB No. 0704-0188

1. AGENCY USE ONLY *(Leave blank)*	2. REPORT DATE	3. REPORT TYPE AND DATES COVERED
	October 1991	Final Jan 89 - Sep 89

4. TITLE AND SUBTITLE

Experimental Measurement of Tailboom Strain During Charge Ignition

5. FUNDING NUMBERS

PR: 1L161102AH43

6. AUTHOR(S)

Joseph W. Colburn and Arthur A. Koszoru

7. PERFORMING ORGANIZATION NAME(S) AND ADDRESS(ES)

8. PERFORMING ORGANIZATION REPORT NUMBER

9. SPONSORING/MONITORING AGENCY NAMES(S) AND ADDRESS(ES)

USA Ballistic Research Laboratory
ATTN: SLCBR-DD-T
Aberdeen Proving Ground, MD 21005-5066

10. SPONSORING/MONITORING AGENCY REPORT NUMBER

BRL-TR-3275

11. SUPPLEMENTARY NOTES

12a. DISTRIBUTION/AVAILABILITY STATEMENT

Approved for Public Release - Distribution is Unlimited

12b. DISTRIBUTION CODE

13. ABSTRACT *(Maximum 200 words)*

The evolution of Armor Piercing Fin Stabilized Discarding Sabot (APFSDS) projectiles has lead to projectiles which protrude substantially into the gun chamber, affecting igniter design, path of flamespread through the charge, and projectile loading. This study focuses on a method of detecting loading of the projectile tailboom during the early phase of the interior ballistic cycle. Using a clear acrylic gun chamber simulator with an instrumented projectile, charge ignition and projectile/charge interactions are observed during the early portion of the ballistic cycle. The projectile tailboom is instrumented with strain gauges to monitor transverse forces. High speed photography and X-rays are used to monitor flame spreading and movement of the charge within the chamber. A microwave interferometer is used to record projectile axial motion. Chamber pressure is monitored with piezoelectric pressure transducers. This report briefly describes the instrumentation and test setup. Data are presented from each test round. These data demonstrate the viability of the strain gage instrumented projectile technique for monitoring projectile/propelling charge interactions during the early portion of the interior ballistic cycle. The initial data are too limited to make general conclusions about the differences in projectile/charge interactions between stick and granular charges, but discernable differences were measured.

14. SUBJECT TERMS

Interior Ballistics, Chamber Simulator, Armor Piercing Projectiles, Strain Gages, Projectile Dynamics

15. NUMBER OF PAGES

26

16. PRICE CODE

17. SECURITY CLASSIFICATION OF REPORT	18. SECURITY CLASSIFICATION OF THIS PAGE	19. SECURITY CLASSIFICATION OF ABSTRACT	20. LIMITATION OF ABSTRACT
UNCLASSIFIED	UNCLASSIFIED	UNCLASSIFIED	SAR

INTENTIONALLY LEFT BLANK

TABLE OF CONTENTS

INTENTIONALLY LEFT BLANK

LIST OF FIGURES

INTENTIONALLY LEFT BLANK

ACKNOWLEDGMENTS

The authors would like to thank Dr. Lang Mann Chang and Dr. Kevin White of the Ballistic Research Laboratory (BRL) for their assistance with the simulator setup. We would also like to thank Carl Ruth, James Bowen, John Hewitt, James Tuerk, and Dennis Meier of BRL's Range18 large caliber gun research facility for their assistance with the firings. Also, special thanks to James Evans of Applied Concepts Corp. for his assistance with the test setup and data analysis, and Robert Phillabaum and David Kruczynski of BRL for their assistance in reviewing this report.

INTENTIONALLY LEFT BLANK

1. INTRODUCTION

Armor Piercing Fin Stabilized Discarding Sabot (APFSDS) projectiles which intrude significantly into the gun chamber have become commonplace in modern tank gun ammunition. At the Ballistic Research Laboratory (BRL), interior ballisticians have developed propelling charges which have continued to push the level of performance despite the increasing intrusion of projectile tailbooms into the gun chamber. Most propelling charge development studies have treated the tailboom as a solid obstacle to be worked around, instead of as a dynamic mechanism which requires "gentle" treatment to preserve the performance of the gun system.

This experiment used projectiles instrumented with strain gauges in transparent acrylic gun chamber simulators to compare the magnitudes of the transverse forces applied to a projectile tailboom during the ignition phase of two different propelling charges.The first charge was based on stick propellant. The second charge used granular propellant.

Stick charges, which are usually packed in a very uniform, radially symmetric fashion generally show little resistance to gas flow in the axial direction, but offer large resistance to radial gas flow (Minor 1988). Large portions of a stick charge are typically bound to the tailboom of an APFSDS projectile. This practice creates radially symmetric regions of ullage which enhance the flame spreading process and generally reinforce the symmetry of the ignition process. Without taking into account any asymmetries caused by the ignition system, the symmetry of the stick charge design yields the intuitive impression that the radial forces applied to the tailboom by the charge during the early ignition phase should be uniform.

Granular charges, which are usually packed in a random fashion, show a uniformly high resistance to gas flow in all directions. Because the propellant is not bound to the projectile it tends to settle during shipping and handling, forming unpredicted ullage regions in the charge. Ullage regions have a very low resistance to gas flow, and can produce unpredictable,asymmetric ignition paths in a charge. By intuition, asymmetric ignition increases the likelyhood of unbalanced loading of the projectile tailboom.

2. SIMULATOR BACKGROUND

Gun chamber simulators are an important tool supporting the development of advanced large caliber gun ammunition at BRL. Simulators generally use a transparent tube, with inside dimensions duplicating the gun chamber under study. This allows the experimenter visual access to events in

the early stages of the interior ballistic cycle. These events include the functioning of the ignition system, flame spreading, and propellant bed motion and compaction. Recently, simulators have been used in the development of low vulnerability charges (Chang 1988), and in the analysis of flame spreading in howitzer charges (Minor and Horst 1986).

There are two basic types of gun chamber simulators used in large caliber interior ballistic studies at BRL. One type is fabricated from transparent acrylic. This allows the use of high speed cameras to record ignition and flame spreading phenomena, as well as propellant bed motion and compaction. The other type of simulator chamber is made of wound fiberglass. This type withstands significantly more pressure before bursting, but it is only transparent to flash X-rays, and translucent to intense light sources (e.g., flame fronts). The limited transparency of the fiberglass wound chamber makes the clear acrylic chamber the most useful choice unless higher maximum pressures are required to observe the phenomena under study.

3. EXPERIMENTAL

3.1 Simulator Instrumentation. Generally, the simulator is instrumented with one or more pressure transducers in the simulator breech, and an array of pressure, acceleration, and force transducers at the rear of the projectile. Video and high speed film cameras can be used to capture the ignition event on film. Flash X-rays are normally taken before (static), and during (dynamic) the ignition to measure movement of the propellant bed or ignition system parts. A displacement measurement device is usually used to detect axial motion of the projectile before chamber failure.

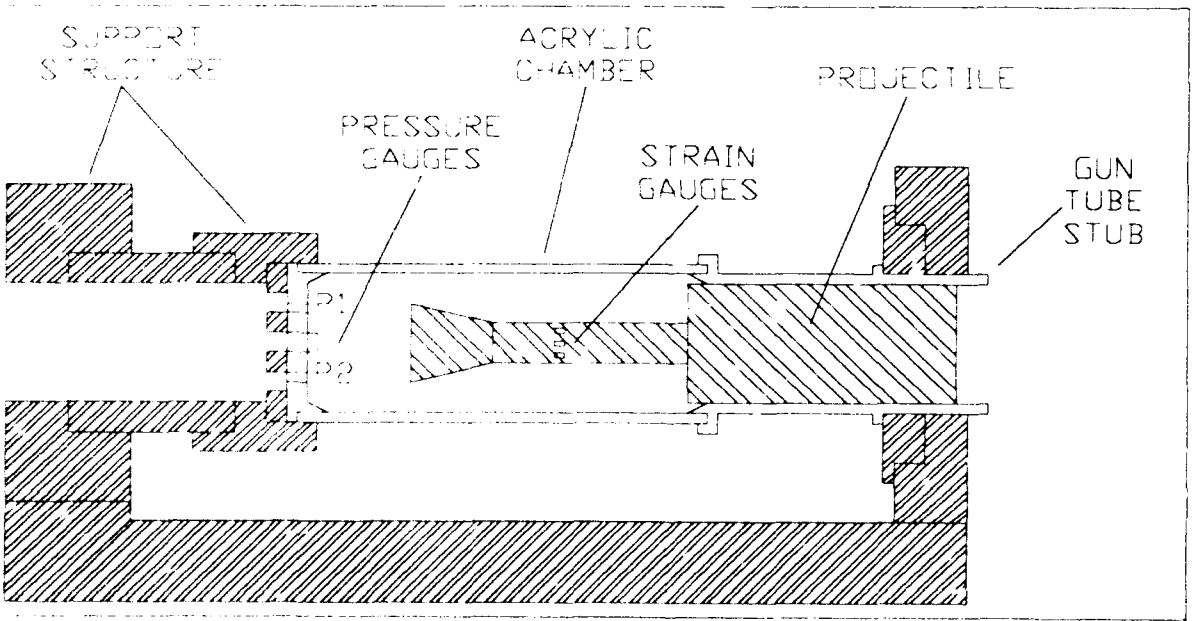

Figure 1. Chamber Simulator Diagram.

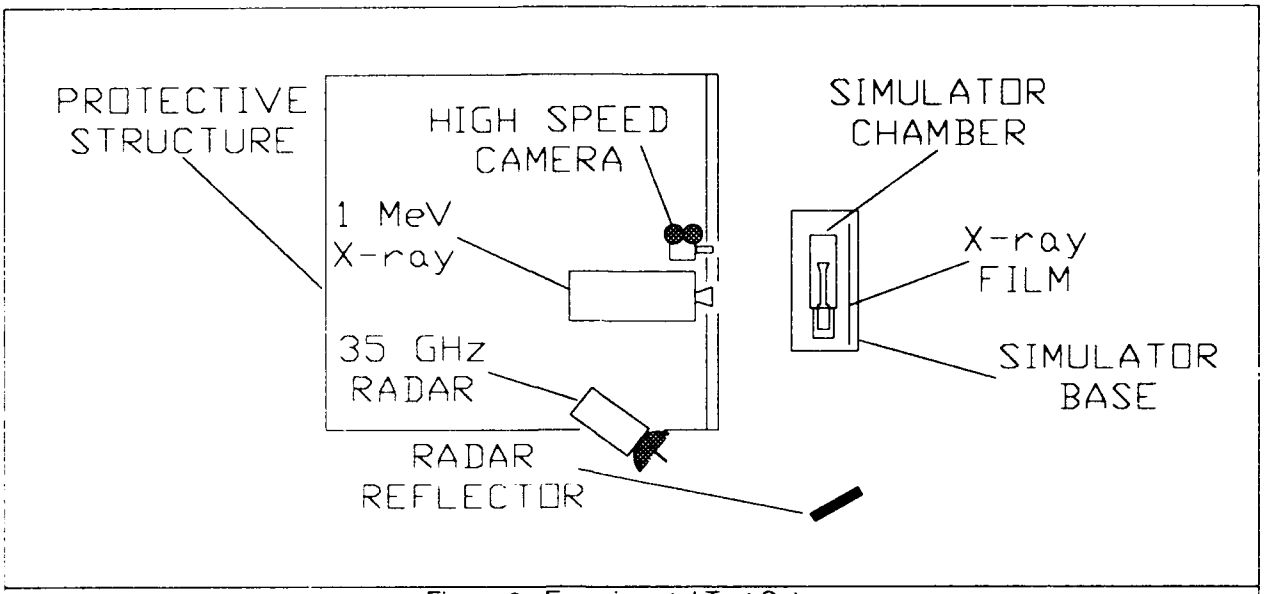

Figure 2. Experimental Test Setup.

Figure 1 presents a cross-sectional view of the transparent acrylic gun chamber simulator used in this experiment. The transparent chamber offered excellent visualization for the recording of the events which occurred inside. The chamber was capable of withstanding dynamic pressures in excess of 15 MPa (2170 psi) before rupturing. The rear end of the chamber was adapted to the base of a real cartridge and its forward end to a short gun barrel in which an instrumented projectile was loaded. The unit was mounted on a steel fixture.

Figure 2 illustrates the experimental arrangement for the simulator diagnostics. The instrumentation used included two pressure gages, six 350 ohm strain gauges, one Photec high speed 16-mm camera, one 1MeV X-ray head, and one 35 GHz TERMA microwave interferometer for measurement of projectile axial displacement .

The pressure gages (quartz PCB Model 113A23) monitored the pressure at the breech end of the chamber. The strain gauges monitored the stress on the projectile tailboom from six radially symmetric locations at the same axial position. The high speed camera monitored flame spreading in the entire chamber. The framing rate of the cameras was set at 5000 frames per second. The X-ray head was positioned on one side of the chamber and a cassette containing Kodak XR-5 film was on the opposite side to record propellant bed motion and compaction. The radar signal was reflected onto the nose of the projectile to record projectile motion as a function of time. The resolution of the 35 GHz radar was 0.4287 cm per interference fringe. Data acquisition and data reduction were performed by the Telemetry Acquisition Reduction and Plotting System (TARPS) at BRL's Sandy Point large caliber firing facility. Data were filtered by a 90 kHz low pass filter to eliminate aliasing before being digitized at 1 MHz.

3.2 Granular Charge. The charge for the granular firing consisted of a modified XM125 bayonet primer and 6.58 kg (14.5 lbs) of JA2, multi-perforated, hexagonal propellant. Before firing, the charge was rotated about its long axis to form a uniform 2 cm ullage at the top of the chamber. This was an attempt to create an asymmetry in the path of flame spreading.

3.3 Stick Charge. The charge for the stick firing consisted of an M123 primer, a doughnut shaped bag containing 100 g (0.22 lbs) of black powder around the primer, and 6.4 kg (14.1 lbs) of JA2 stick propellant. The majority of the stick propellant (4.13 kg (9.1 lbs)) was stacked symmetrically around the tailboom (long axis of the propellant parallel with the long axis of the projectile)and secured with packing tape. The remaining 2.27 kg (5 lbs) of propellant was stacked in a cylindrical shape, taped together, and placed in the chamber behind the projectile. X-ray data showed that the 2.27 kg charge increment was offset from the main portion of the charge by 1 cm before firing.

4. DATA ANALYSIS

The following data are by no means generic to the types of charges used. The intent of this two round study was to verify the viability of the experimental techniques and to point out methods of improving future experiments.

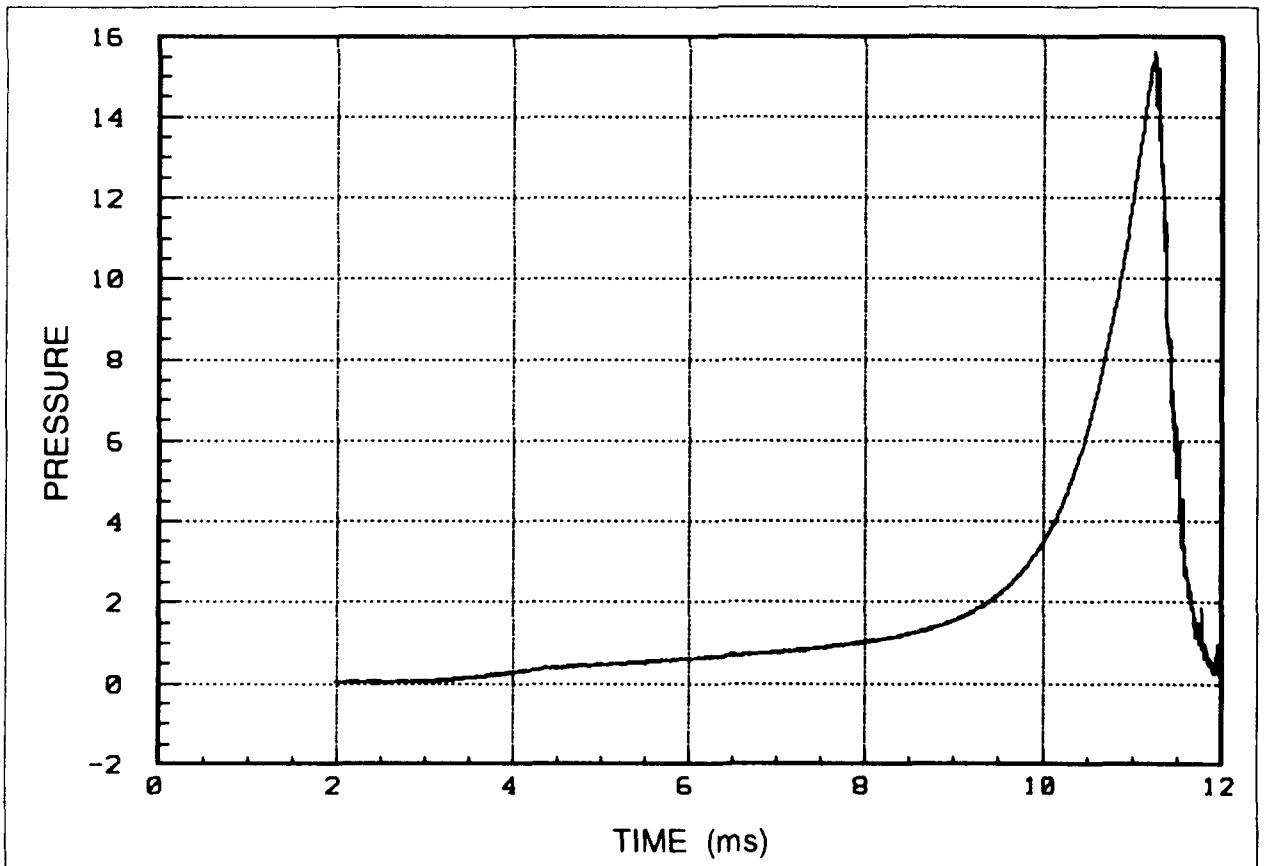

Figure 3. Granular Charge Breech Pressure.

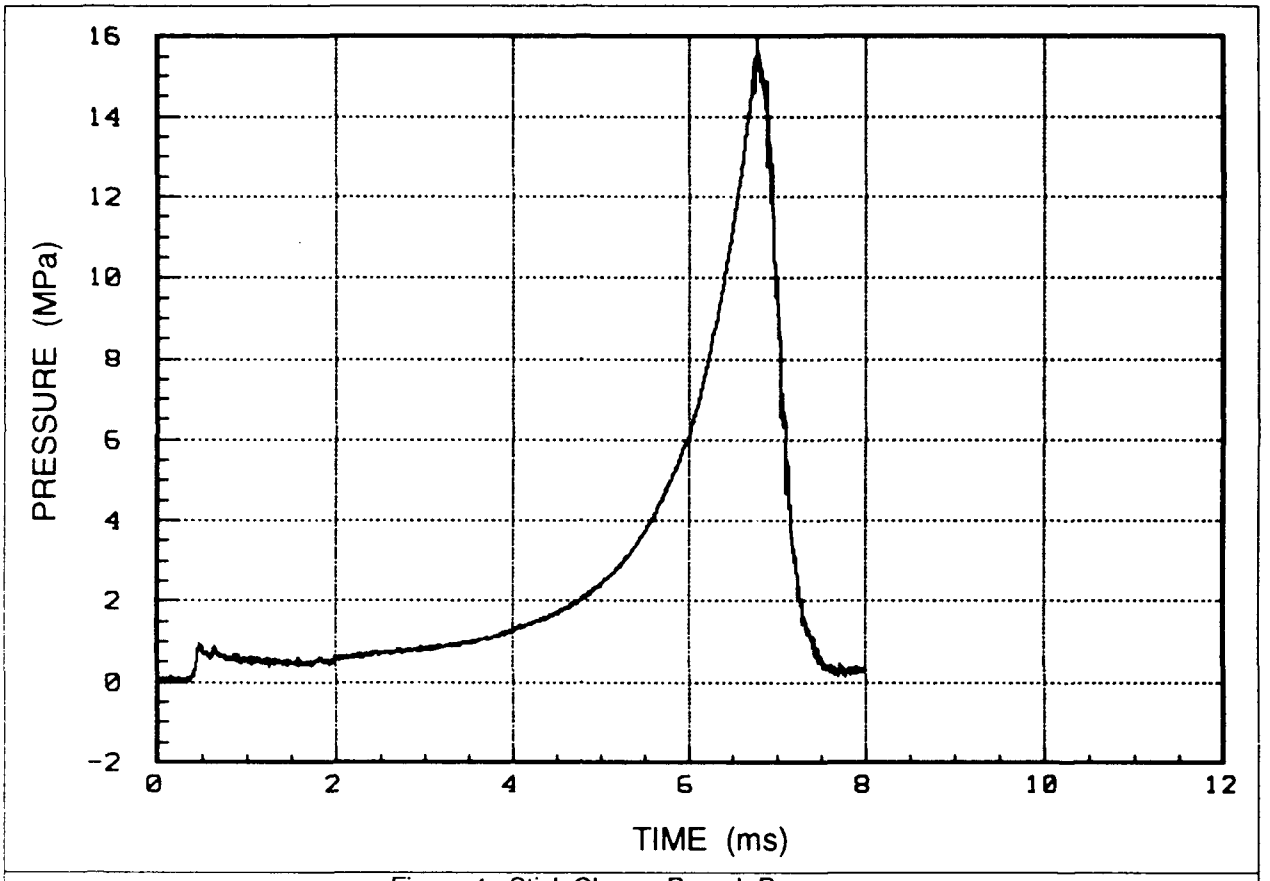

Figure 4. Stick Charge Breech Pressure.

4.1 Pressure Time Histories. Figure 3 shows the pressure time history for the granular round. The chamber ruptured at 15.5 MPa (2250 psi), 11.2 ms after application of the firing pulse. The pressure rise appeared to be smooth, without noticeable aberration. The bayonet primer vented into the center of the propellant bed so the breech mounted pressure gauges did not detect a pressure spike at the time of primer function. Since there were no pressure gauges at the forward end of the chamber no pressure wave analysis could be attempted. For purposes of clarity only the data from one pressure transducer are shown in the plots. In all cases the data from the other transducer are nearly identical to the data shown.

Figure 4 shows the pressure time history for the stick round. The chamber ruptured at 15.5 MPa (2250 psi), 6.8 ms after application of the firing pulse. A spike was observed on the pressure time history corresponding to the functioning of the M123 primer and combustion of the black powder bag. The ullage region at the rear of the propelling charge, where the ignition elements were located, was adjacent to the pressure transducers mounted in the stub base. This arrangement allowed the pressure transducers to respond immediately to the ignition pulse.

Except for the evidence of primer function on the stick charge pressure time history the only significant difference between the granular and stick charge pressure traces was the time delay before chamber rupture. It is possible that the low axial flow resistance of the stick charge allowed it to ignite more quickly, and burst the simulator 4.4 ms before the granular charge.

4.2 Radar Data. Figures 5 and 6 show the distance and velocity histories of the granular round. The projectile had moved 3.25 cm and was traveling at 15 m/s at the time of chamber rupture (11.2 ms). Figures 7 and 8 show the distance and velocity histories of the stick round. The projectile had moved 3.40 cm and was traveling at 30 m/s at the time of chamber rupture (6.8 ms).

The higher projectile velocity attained in a shorter time by the stick charge shows the effects of the lower resistance to axial gas flow as compared to the granular charge. It should also be noted that, in this case, greater acceleration places more stress on the projectile.

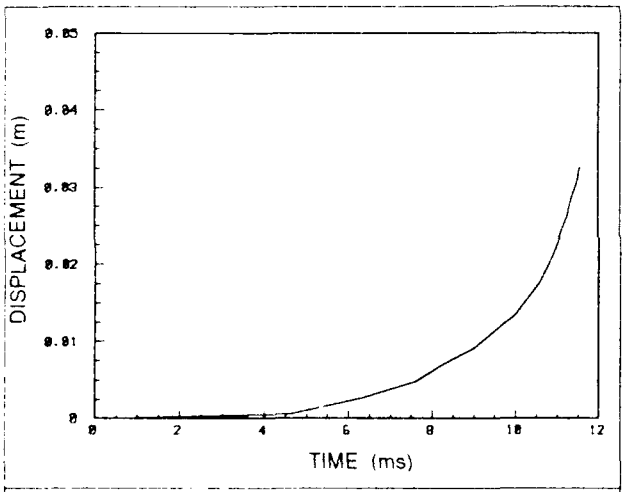

Figure 5. Granular Charge Displacement.

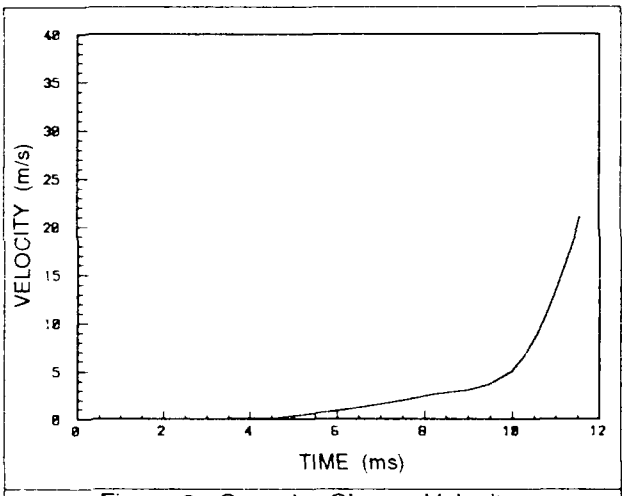

Figure 6. Granular Charge Velocity.

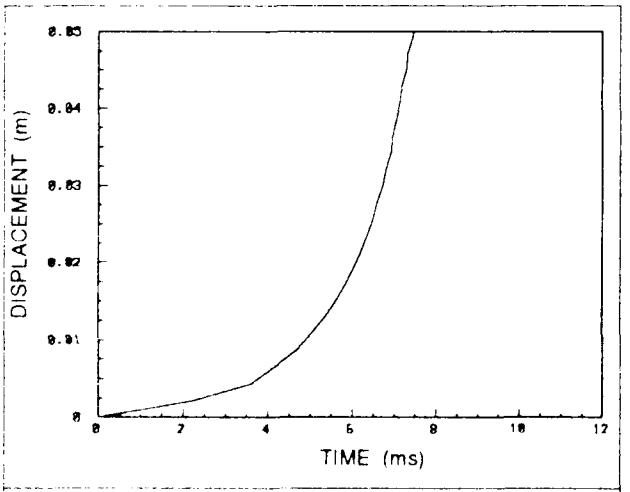

Figure 7. Stick Charge Displacement.

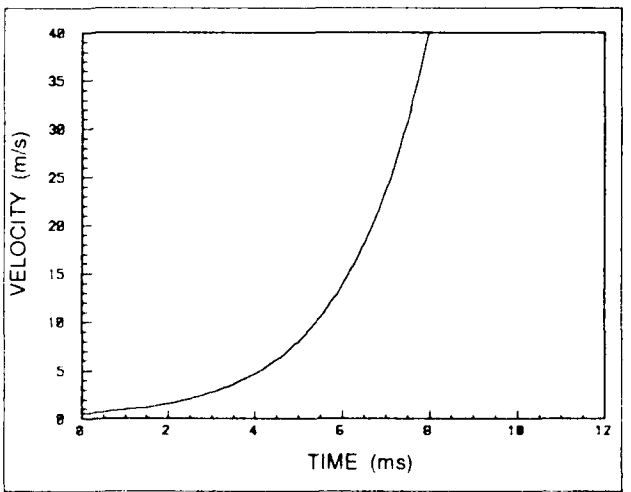

Figure 8. Stick Charge Velocity.

4.3 Strain Records. Figure 9 shows the strain histories for the granular charge. Data shown for diametrically opposite strain gauges account for approximately equal, but opposite peaks. The first major peak (at 4 ms) shows the beginning of oscillatory strains on the tailboom. These strains were probably due to propellant bed compaction resulting from primer function. Notice that the strains have settled at 7 ms, indicating that the propellant bed was fully compacted. The peak at 8 ms corresponds to a change in the slope of the pressure time history (Figure 3) which indicated ignition of the main charge. This was the beginning of a second set of strain oscillations in the tailboom which terminated at chamber rupture.

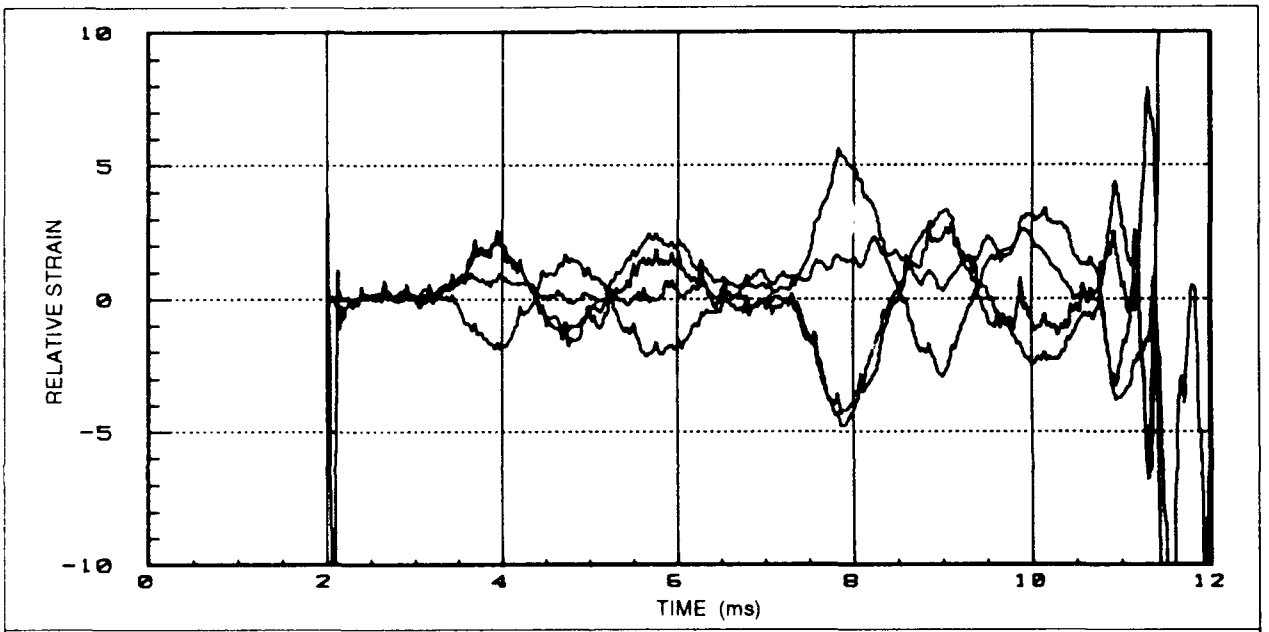

Figure 9. Granular Charge Strain.

It was desired to evaluate the strain data to determine the angular location of the peak strain value, and the magnitude of the peak strain. It was acknowledged that this analysis would only be valid for the axial location common to the strain transducers under study.

If it is assumed that the magnitude of axial strain in the tailboom of a projectile falls off linearly with respect to angle, then the magnitude and angle of the principal strain axis of the tailboom can be determined at any point in time by evaluating the strain histories from two transducers which were not on the same radial axis. The analysis is executed by expressing the two measured strain data sets in terms of a projection of a strain of unknown magnitude which is at a maximum at an unknown angle from each strain measurement position. Since the angle between the strain measurement positions is known we are left with two equations and two unknowns. The simultaneous solution for the axis angle is substituted back into the original equations to determine the

magnitude of strain on that axis. This calculation is performed for each point in the strain-time histories. Appendix A details the mathematical manipulations.

Figures 10 and 11 display calculated values for the orientation of the axis of maximum strain (parallel to the bending axis of the tail boom) and the absolute magnitude of the strain that would have been measured on that axis if a transducer had been placed there. Each plot contains three separate data sets. These correspond to evaluation of the 0°, 60° pair, the 0°, 120° pair, and the 60°, 120°pair of strain records. If the axis of maximum strain had not moved during the test the plot of axis direction versus time would appear as a square wave, with the angle shifting by 180° each time the strain passes through zero. As shown for the granular charge the axis of maximum strain seems to have moved from horizontal oscillations, to near vertical oscillations, then switched back to horizontal just before the chamber ruptured. It should be noted that if at any time the axis of maximum strain was perpendicular to the angular midpoint between the transducer pair under

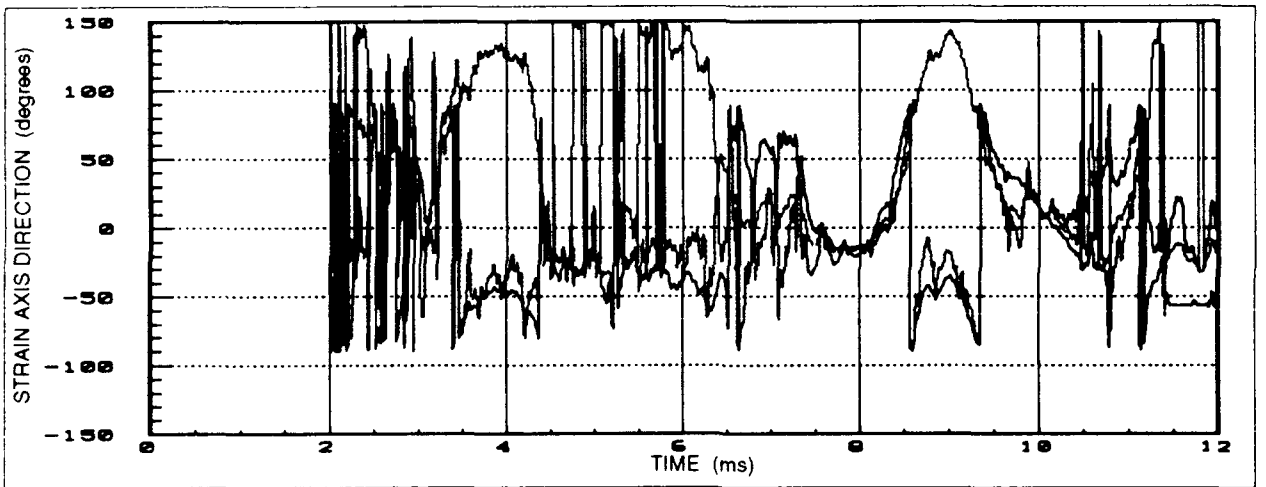

Figure 10. Granular Charge, Strain Axis Direction.

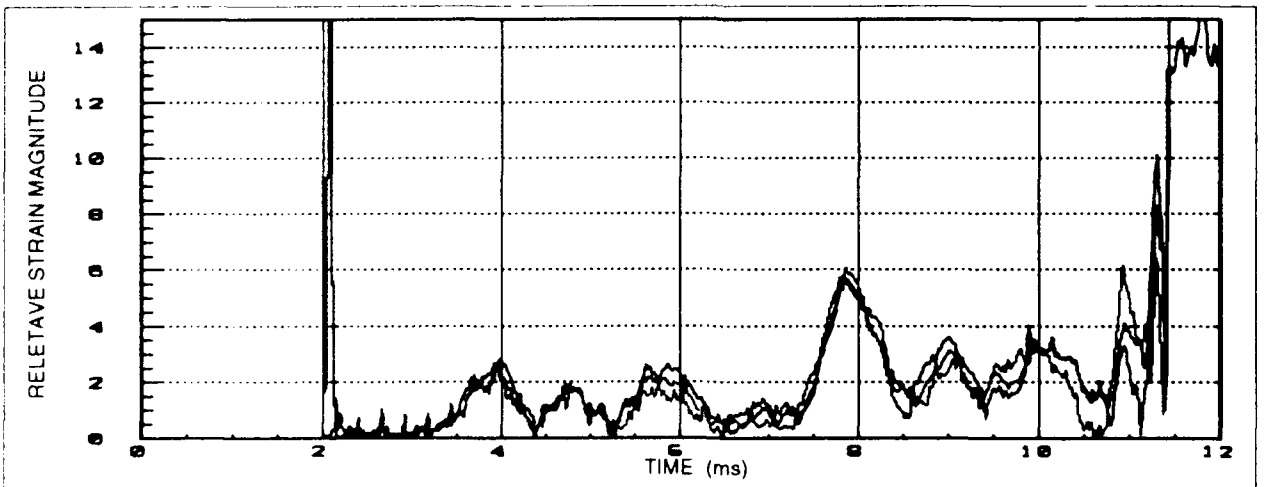

Figure 11. Granular Charge, Strain Magnitude.

evaluation, the axis direction calculation wouldn't show a zero crossing at that instant because it was on a null point. This occurred several times in the evaluation of the 60°, 120° pair. That trace stands out in Figure 10 because it remains above the 90° level while the other two traces show direction reversals.

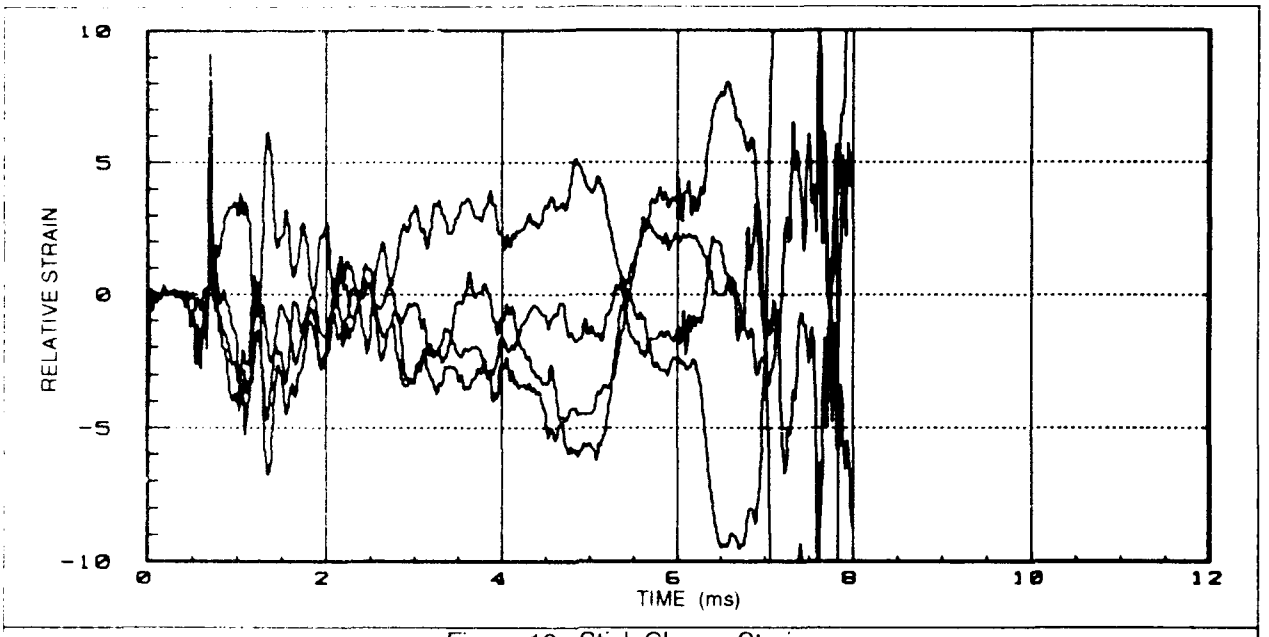

Figure 12. Stick Charge Strain.

Figure 12 shows the strain histories for the stick charge. The very large peak at 1 ms was electronic noise as indicated by the fact that all of the strain gauges responded in the same direction. Overall, the stick charge strain history showed oscillatory behavior similar to the granular charge, but at a much higher frequency. The first significant peak (1.5 ms) was probably due to the impact of the 2.27 kg charge increment on the main charge. The strain peak at 5 ms corresponded to the

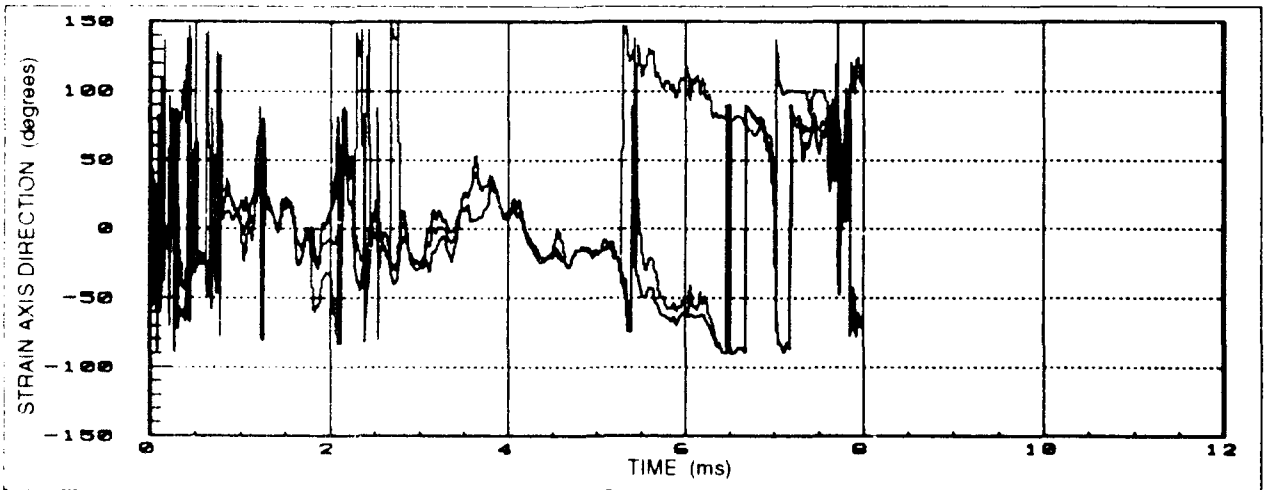

Figure 13. Stick Charge, Strain Axis Direction.

slope change in the pressure time history shown in Figure 4. This slope change indicated the ignition of the main charge. The large strain peak after 6 ms in Figures 12 and 14 occurred after chamber rupture and was not considered significant. Figures 13 and 14 show the calculations for principal strain axis and strain magnitude as detailed previously. The data set pairs evaluated for this round were the 0°, 60° pair, the 0°, 300° pair, and the 60°, 300° pair.

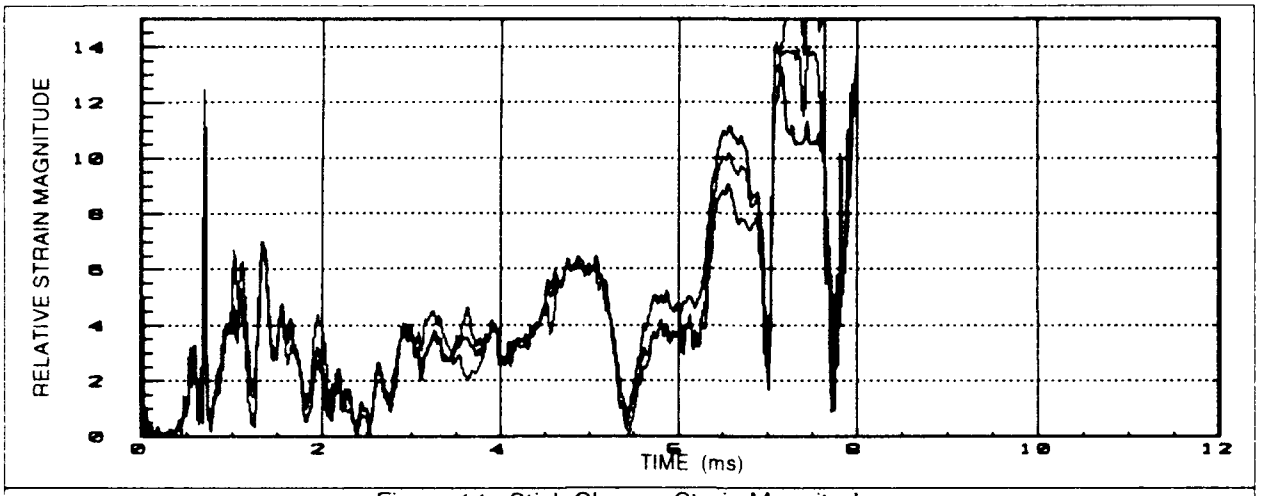

Figure 14. Stick Charge, Strain Magnitude.

5. CONCLUSIONS

The combination of plastic chamber simulators and strain gauge instrumented projectiles provides an opportunity to make unique measurements of charge/projectile interactions during the early phase of charge ignition. This type of system could be used to evaluate candidate propelling charges for detrimental effects on projectiles, as well as studying ignition anomalies caused by charge geometry. An instrumented tail boom can be a sensitive, yet robust transducer for data collection in the interior ballistic environment.

The success of these test firings indicates that this method of projectile instrumentation is indeed a viable method of recording transverse forces on projectile tailbooms in the early phase of charge ignition.

Although the limited scope of this test prevents the drawing of any general conclusions about the differences in propellant/tailboom interactions during the ignition phase of granular and stick charges, it does show that each charge has measurably different interactions with the tailboom. Future applications of this technique should be optimized to study specific projectile/charge systems or particular ignition asymmetries in each type of charge.

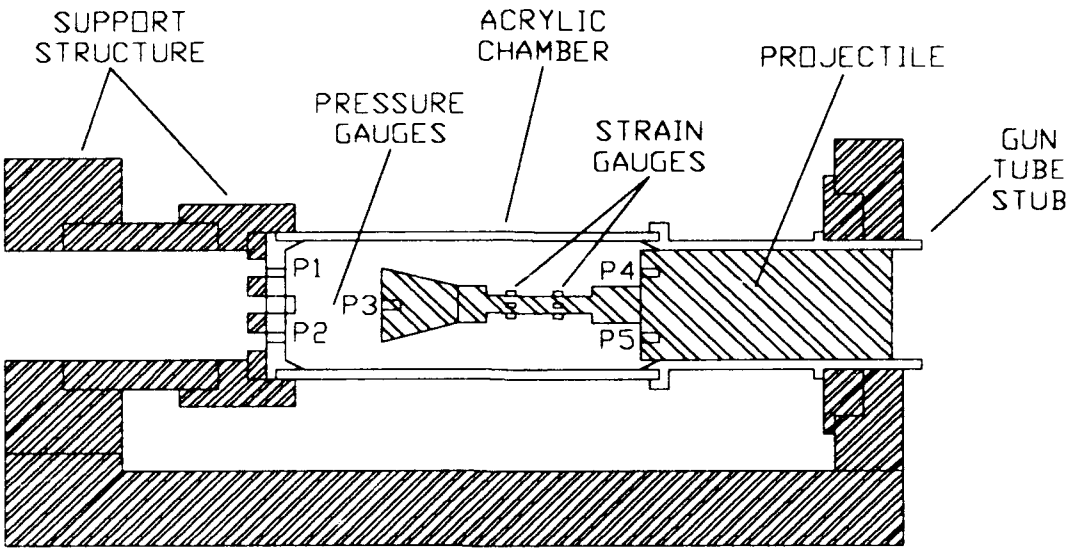

Figure 15. Modified Simulator Setup.

To accurately compare data between different charges and loading asymmetries a common projectile should be used. Figure 15 shows a sketch of a projectile which would be better suited for such a purpose. The pressure gauges mounted in the projectile would allow analysis of ignition induced pressure waves. Locating the strain gauges on a thinned down section of the tailboom would make the system more sensitive to asymmetric forces. An increased number of strain gauges combined with finite element analysis of the test projectile could allow the strain data from a generic projectile to be applied to specific systems under study.

6. REFERENCES

Chang, L-M. "Pressure-Flamespread Correlations In the Simulator Ignition Studies of 105-mm Tank Charges." BRL-TR-2891, U.S. Army Ballistic Research Laboratory, Aberdeen Proving Ground, MD, March 1988.

Minor, T.C. "Flamespreading Processes in Obliquely Loaded Stick Propellant Beds." BRL-TR-2894, U.S. Army Ballistic Research Laboratory, Aberdeen Proving Ground, MD, March 1988.

Minor, T.C., and A.W. Horst, "Theoretical and Experimental Investigation of Flamespreading Processes in Combustible-Cased, Stick Propellant Charges." BRL-TR-2710, U.S. Army Ballistic Research Laboratory, Aberdeen Proving Ground, MD, February 1986.

INTENTIONALLY LEFT BLANK

APPENDIX.

PROCEDURE FOR REDUCING STRAIN DATA

INTENTIONALLY LEFT BLANK

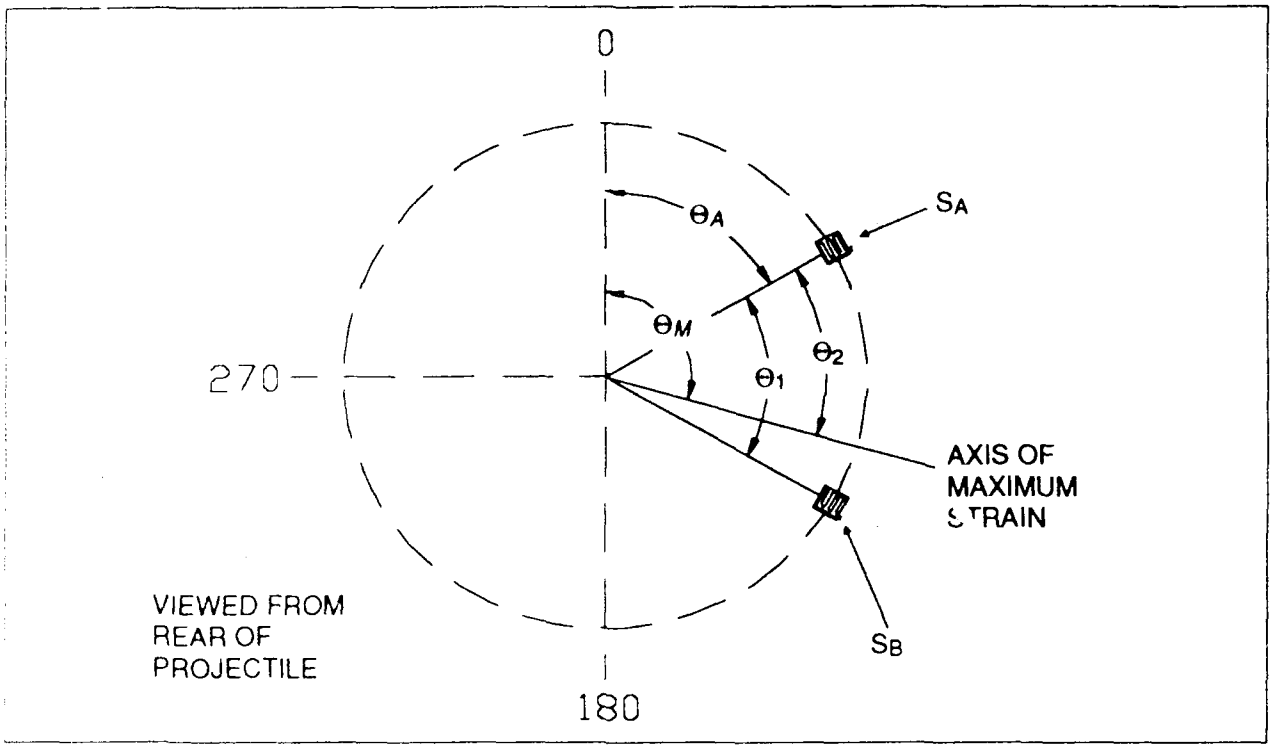

Equations A.1 through A.8 detail the procedure used to produce the data shown in Figures 10, 11, 13, and 14 in this report. The reader is referred to the diagram above to explain the angular references made in the equations.

Given: M_A and M_B are instantaneous strain magnitudes measured at non-radially-aligned transducer locations S_A and S_B. The angle between the two transducers is defined as Θ_1, the angle between S_A and the axis of maximum strain is defined as Θ_2., and the angle from top-dead-center to S_A is defined as Θ_A. The computed magnitude of maximum strain is represented as M_M, and the angle of the axis of maximum strain is Θ_M.

Our purpose is to solve for M_M and Θ_M

Given:

$$\Theta_M = \Theta_A + \Theta_2 \qquad \text{(A.1)}$$

$$M_A = M_M \cos\Theta_2 \qquad \text{(A.2)}$$

$$M_B = M_M \cos(\Theta_2 - \Theta_1) \qquad \text{(A.3)}$$

Therefore:

$$\frac{M_B}{M_A} = \frac{\cos(\Theta_2 - \Theta_1)}{\cos\Theta_2} \qquad \text{(A 4)}$$

$$\frac{M_B}{M_A} = \frac{\cos\Theta_2 \ \cos\Theta_1 + \sin\Theta_2 \cos\Theta_1)}{\cos\Theta_2} \qquad \text{(A 5)}$$

$$\frac{M_B}{M_A} = \cos\Theta_1 + \sin\Theta_1 \ \tan\Theta_2 \qquad \text{(A 6)}$$

$$arctan\left(\frac{\frac{M_B}{M_A} - \cos\Theta_1}{\sin\Theta_1}\right) = \Theta_2 \qquad \text{(A 7)}$$

Therefore:

$$\Theta_M = arctan\left(\frac{\frac{M_B}{M_A} - \cos\Theta_1}{\sin\Theta_1}\right) + \Theta_A \qquad \text{(A 8)}$$

No. of Copies	Organization
2	Administrator Defense Technical Info Center ATTN: DTIC-DDA Cameron Station Alexandria, VA 22304-6145
1	Commander U.S. Army Materiel Command ATTN: AMCDRA-ST 5001 Eisenhower Avenue Alexandria, VA 22333-0001
1	Commander U.S. Army Laboratory Command ATTN: AMSLC-DL 2800 Powder Mill Road Adelphi, MD 20783-1145
2	Commander U.S. Army Armament Research, Development, and Engineering Center ATTN: SMCAR-IMI-I Picatinny Arsenal, NJ 07806-5000
2	Commander U.S. Army Armament Research, Development, and Engineering Center ATTN: SMCAR-TDC Picatinny Arsenal, NJ 07806-5000
1	Director Benet Weapons Laboratory U.S. Army Armament Research, Development, and Engineering Center ATTN: SMCAR-CCB-TL Watervliet, NY 12189-4050
(Unclass. only)1	Commander U.S. Army Armament, Munitions and Chemical Command ATTN: AMSMC-IMF-L Rock Island, IL 61299-5000
1	Director U.S. Army Aviation Research and Technology Activity ATTN: SAVRT-R (Library) M/S 219-3 Ames Research Center Moffett Field, CA 94035-1000

No. of Copies	Organization
1	Commander U.S. Army Missile Command ATTN: AMSMI-RD-CS-R (DOC) Redstone Arsenal, AL 35898-5010
1	Commander U.S. Army Tank-Automotive Command ATTN: ASQNC-TAC-DIT (Technical Information Center) Warren, MI 48397-5000
1	Director U.S. Army TRADOC Analysis Command ATTN: ATRC-WSR White Sands Missile Range, NM 88002-5502
1	Commandant U.S. Army Field Artillery School ATTN: ATSF-CSI Ft. Sill, OK 73503-5000
(Class. only)1	Commandant U.S. Army Infantry School ATTN: ATSH-CD (Security Mgr.) Fort Benning, GA 31905-5660
(Unclass. only)1	Commandant U.S. Army Infantry School ATTN: ATSH-CD-CSO-OR Fort Benning, GA 31905-5660
1	Air Force Armament Laboratory ATTN: WL/MNOI Eglin AFB, FL 32542-5000
	Aberdeen Proving Ground
2	Dir, USAMSAA ATTN: AMXSY-D AMXSY-MP, H. Cohen
1	Cdr, USATECOM ATTN: AMSTE-TC
3	Cdr, CRDEC, AMCCOM ATTN: SMCCR-RSP-A SMCCR-MU SMCCR-MSI
1	Dir, VLAMO ATTN: AMSLC-VL-D
10	Dir, BRL ATTN: SLCBR-DD-T

No. of Copies	Organization
1	Commander U.S. Army Concepts Analysis Agency ATTN: D. Hardison 8120 Woodmont Ave. Bethesda, MD 20014
1	C.I.A. 01R/DB/Standard Washington, DC 20505
1	Director U.S. Army Ballistic Missile Defense Systems Command Advanced Technology Center P. O. Box 1500 Huntsville, AL 35807-3801
1	Chairman DOD Explosives Safety Board Room 856-C Hoffman Bldg. 1 2461 Eisenhower Ave. Alexandria, VA 22331-0600
1	Commander U.S. Army Materiel Command ATTN: AMCDE-DW 5001 Eisenhower Ave. Alexandria, VA 22333-5001
1	Department of the Army Office of the Product Manager 155mm Howitzer, M109A6, Paladin ATTN: SFAE-AR-HIP-IP, Mr. R. De Kleine Picatinny Arsenal, NJ 07806-5000
2	Commander Production Base Modernization Agency U.S. Army Armament Research, Development, and Engineering Center ATTN: AMSMC-PBM, A. Siklosi AMSMC-PBM-E, L. Laibson Picatinny Arsenal, NJ 07806-5000

No. of Copies	Organization
3	PEO-Armaments Project Manager Tank Main Armament Systems ATTN: AMCPM-TMA, K. Russell AMCPM-TMA-105 AMCPM-TMA-120, C. Roller Picatinny Arsenal, NJ 07806-5000
15	Commander U.S. Army Armament Research, Development, and Engineering Center ATTN: SMCAR-AEE SMCAR-AEE-B, A. Beardell D. Downs S. Einstein S. Westley S. Bernstein J. Rutkowski B. Brodman P. Bostonian R. Cirincione A. Grabowsky P. Hui J. O'Reilly N. Ross SMCAR-AES, S. Kaplowitz Picatinny Arsenal, NJ 07806-5000
2	Commander U.S. Army Armament Research, Development, and Engineering Center ATTN: SMCAR-CCD, D. Spring SMCAR-CCH-V, C. Mandala Picatinny Arsenal, NJ 07806-5000
1	Commander U.S. Army Armament Research, Development, and Engineering Center ATTN: SMCAR-HFM, E. Barrieres Picatinny Arsenal, NJ 07806-5000
1	Commander U.S. Army Armament Research, Development, and Engineering Center ATTN: SMCAR-FSA-T, M. Salsbury Picatinny Arsenal, NJ 07806-5000

No. of Copies	Organization
1	Commander, USACECOM R&D Technical Library ATTN: ASQNC-ELC-IS-L-R, Myer Center Fort Monmouth, NJ 07703-5301
1	Commander U.S. Army Harry Diamond Laboratories ATTN: SLCHD-TA-L 2800 Powder Mill Rd. Adelphi, MD 20783-1145
1	Commandant U.S. Army Aviation School ATTN: Aviation Agency Fort Rucker, AL 36360
2	Program Manager U.S. Tank-Automotive Command ATTN: AMCPM-ABMS, T. Dean (2 cps) Warren, MI 48092-2498
1	Program Manager U.S. Tank-Automotive Command Fighting Vehicles Systems ATTN: AMCPM-BFVS Warren, MI 48092-2498
1	President U.S. Army Armor & Engineer Board ATTN: ATZK-AD-S Fort Knox, KY 40121
1	Project Manager U.S. Army Tank-Automotive Command M-60 Tank Development ATTN: AMCPM-ABMS Warren, MI 48092-2498
1	Director HQ, TRAC RPD ATTN: ATCD-MA Fort Monroe, VA 23651-5143
2	Director U.S. Army Materials Technology Laboratory ATTN: SLCMT-ATL (2 cps) Watertown, MA 02172-0001

No. of Copies	Organization
1	Commander U.S. Army Research Office ATTN: Technical Library P.O. Box 12211 Research Triangle Park, NC 27709-2211
1	Commander U.S. Army Belvoir Research and Development Center ATTN: STRBE-WC Fort Belvoir, VA 22060-5006
1	Director U.S. Army TRAC-Ft. Lee ATTN: ATRC-L, Mr. Cameron Fort Lee, VA 23801-6140
1	Commandant U.S. Army Command and General Staff College Fort Leavenworth, KS 66027
1	Commandant U.S. Army Special Warfare School ATTN: Rev and Trng Lit Div Fort Bragg, NC 28307
3	Commander Radford Army Ammunition Plant ATTN: SMCAR-QA/HI LIB (3 cps) Radford, VA 24141-0298
1	Commander U.S. Army Foreign Science and Technology Center ATTN: AMXST-MC-3 220 Seventh Street, NE Charlottesville, VA 22901-5396
2	Commander Naval Sea Systems Command ATTN: SEA 62R SEA 64 Washington, DC 20362-5101
1	Commander Naval Air Systems Command ATTN: AIR-954-Technical Library Washington, DC 20360

No. of Copies | Organization

1 Assistant Secretary of the Navy
(R, E, and S)
ATTN: R. Reichenbach
Room 5E787
Pentagon Bldg
Washington, DC 20375

1 Naval Research Laboratory
Technical Library
Washington, DC 20375

2 Commandant
U.S. Army Field Artillery Center
and School
ATTN: ATSF-CO-MW, E. Dublisky (2 cps)
Fort Sill, OK 73503-5600

1 Office of Naval Research
ATTN: Code 473, R. S. Miller
800 N. Quincy Street
Arlington, VA 22217-9999

3 Commandant
U.S. Army Armor School
ATTN: ATZK-CD-MS, M. Falkovitch (3 cps)
Armor Agency
Fort Knox, KY 40121-5215

2 Commander
U.S. Naval Surface Warfare Center
ATTN: J. P. Consaga
C. Gotzmer
Indian Head, MD 20640-5000

3 Commander
Naval Surface Warfare Center
ATTN: Code 730
Code R-13,
K. Kim
R. Bernecker
10901 New Hampshire Ave.
Silver Spring, MD 20903-5000

No. of Copies | Organization

2 Commanding Officer
Naval Underwater Systems Center
ATTN: Code 5B331, R. S. Lazar
Technical Library
Newport, RI 02840

5 Commander
Naval Surface Warfare Center
ATTN: Code G33,
J. L. East
W. Burrell
J. Johndrow
Code G23, D. McClure
Code DX-21 Technical Library
Dahlgren, VA 22448-5000

3 Commander
Naval Weapons Center
ATTN: Code 388, C. F. Price
Code 3895, T. Parr
Information Science Division
China Lake, CA 93555-6001

1 OSD/SDIO/IST
ATTN: Dr. Len Caveny
Pentagon
Washington, DC 20301-7100

3 Commander
Naval Ordnance Station
ATTN: T. C. Smith
D. Brooks
Technical Library
Indian Head, MD 20640-5000

1 AL/TSTL (Technical Library)
ATTN: J. Lamb
Edwards AFB, CA 93523-5000

1 AFATL/DLYV
Eglin AFB, FL 32542-5000

1 AFATL/DLXP
Eglin AFB, FL 32542-5000

1 AFATL/DLJE
Eglin AFB, FL 32542-5000

No. of Copies | Organization

1 NASA/Lyndon B. Johnson Space Center
ATTN: NHS-22 Library Section
Houston, TX 77054

1 AFELM, The Rand Corporation
ATTN: Library D
1700 Main Street
Santa Monica, CA 90401-3297

3 AAI Corporation
ATTN: J. Hebert
J. Frankle
D. Cleveland
P.O. Box 126
Hunt Valley, MD 21030-0126

2 Aerojet Solid Propulsion Company
ATTN: P. Micheli
L. Torreyson
Sacramento, CA 96813

1 Atlantic Research Corporation
ATTN: M. King
5390 Cherokee Ave.
Alexandria, VA 22312-2302

3 AL/LSCF
ATTN: J. Levine
L. Quinn
T. Edwards
Edwards AFB, CA 93523-5000

1 AVCO Everett Research Laboratory
ATTN: D. Stickler
2385 Revere Beach Parkway
Everett, MA 02149-5936

2 Calspan Corporation
ATTN: C. Murphy (2 cps)
P.O. Box 400
Buffalo, NY 14225-0400

1 General Electric Company
Tactical Systems Department
ATTN: J. Mandzy
100 Plastics Ave.
Pittsfield, MA 01201-3698

No. of Copies | Organization

1 IITRI
ATTN: M. J. Klein
10 W. 35th Street
Chicago, IL 60616-3799

1 Hercules, Inc.
Allegheny Ballistics Laboratory
ATTN: William B. Walkup
P.O. Box 210
Rocket Center, WV 26726

1 Hercules, Inc.
Radford Army Ammunition Plant
ATTN: E. Hibshman
Radford, VA 24141-0299

3 Director
Lawrence Livermore National Laboratory
ATTN: L-355,
A. Buckingham
M. Finger
L-324, M. Constantino
P.O. Box 808
Livermore, CA 94550-0622

1 Olin Corporation
Badger Army Ammunition Plant
ATTN: F. E. Wolf
Baraboo, WI 53913

3 Olin Ordnance
ATTN: E. J. Kirschke
A. F. Gonzalez
D. W. Worthington
P.O. Box 222
St. Marks, FL 32355-0222

1 Paul Gough Associates, Inc.
ATTN: Dr. Paul S. Gough
1048 South Street
Portsmouth, NH 03801-5423

1 Physics International Company
ATTN: Library, H. Wayne Wampler
2700 Merced Street
San Leandro, CA 98457-5602

No. of
Copies Organization

1 Princeton Combustion Research
Laboratory, Inc.
ATTN: M. Summerfield
475 U.S. Highway One
Monmouth Junction, NJ 08852-9650

2 Rockwell International
Rocketdyne Division
ATTN: BA08,
J.E. Flanagan
J. Gray
6633 Canoga Ave.
Canoga Park, CA 91303-2703

1 Thiokol Corporation
Huntsville Division
ATTN: Technical Library
Huntsville, AL 35807

1 Sverdrup Technology, Inc.
ATTN: Dr. John Deur
2001 Aerospace Parkway
Brook Park, OH 44142

2 Thiokol Corporation
Elkton Division
ATTN: R. Biddle
Technical Library
P.O. Box 241
Elkton, MD 21921-0241

1 Veritay Technology, Inc.
ATTN: E. Fisher
4845 Millersport Highway
East Amherst NY 14501-0305

1 Universal Propulsion Company
ATTN: H. J. McSpadden
Black Canyon Stage 1
Box 1140
Phoenix, AZ 84029

1 Battelle
ATTN: TACTEC Library, J N. Huggins
505 King Ave.
Columbus, OH 43201-2693

No. of
Copies Organization

1 Brigham Young University
Department of Chemical Engineering
ATTN: M. Beckstead
Provo, UT 84601

1 California Institute of Technology
204 Karman Laboratory
Main Stop 301-46
ATTN: F.E.C. Culick
1201 E. California Street
Pasadena, CA 91109

1 California Institute of Technology
Jet Propulsion Laboratory
ATTN: L. D. Strand, MS 512/102
4800 Oak Grove Drive
Pasadena, CA 91109-8099

1 University of Illinois
Department of Mechanical/Industrial
Engineering
ATTN: H. Krier
144 MEB; 1206 N. Green Street
Urbana, IL 61801-2978

1 University of Massachusetts
Department of Mechanical Engineering
ATTN: K. Jakus
Amherst, MA 01002-0014

1 University of Minnesota
Department of Mechanical Engineering
ATTN: E. Fletcher
Minneapolis, MN 55414-3368

3 Georgia Institute of Technology
School of Aerospace Engineering
ATTN: B.T. Zinn
E. Price
W.C. Strahle
Atlanta, GA 30332

1 Institute of Gas Technology
ATTN: D. Gidaspow
3424 S. State Street
Chicago, IL 60616-3896

No. of Copies	Organization
1	Johns Hopkins University Applied Physics Laboratory Chemical Propulsion Information Agency ATTN: T. Christian Johns Hopkins Road Laurel, MD 20707-0690
1	Massachusetts Institute of Technology Department of Mechanical Engineering ATTN: T. Toong 77 Massachusetts Ave. Cambridge, MA 02139-4307
1	Pennsylvania State University Applied Research Laboratory ATTN: G. M. Faeth University Park, PA 16802-7501
1	Pennsylvania State University Department of Mechanical Engineering ATTN: K. Kuo University Park, PA 16802-7501
1	Purdue University School of Mechanical Engineering ATTN: J. R. Osborn TSPC Chaffee Hall West Lafayette, IN 47907-1199
1	SRI International Propulsion Sciences Division ATTN: Technical Library 333 Ravenwood Ave. Menlo Park, CA 94025-3493
1	Rensselaer Ploytechnic Institute Department of Mathematics Troy, NY 12181
2	Director Los Alamos Scientific Laboratory ATTN: T3, D. Butler M. Division, B. Craig P.O. Box 1663 Los Alamos, NM 87544

No. of Copies	Organization
1	General Applied Sciences Laboratory ATTN: J. Erdos 77 Raynor Ave. Ronkonkama, NY 11779-6649
1	Battelle PNL ATTN: Mr. Mark Garnich P.O. Box 999 Richland, WA 99352
1	Stevens Institute of Technology Davidson Laboratory ATTN: R. McAlevy, III Castle Point Station Hoboken, NJ 07030-5907
1	Rutgers University Department of Mechanical and Aerospace Engineering ATTN: S. Temkin University Heights Campus New Brunswick, NJ 08903
1	University of Southern California Mechanical Engineering Department ATTN: 0HE200, M. Gerstein Los Angeles, CA 90089-5199
2	University of Utah Department of Chemical Engineering ATTN: A. Baer G. Flandro Salt Lake City, UT 84112-1194
1	Washington State University Department of Mechanical Engineering ATTN: C. T. Crowe Pullman, WA 99163-5201
1	Alliant Techsystems, Inc. ATTN: R. E. Tompkins MN38-3300 5700 Smetana Drive Minnetonka, MN 55343
1	Science Applications, Inc. ATTN: R. B. Edelman 23146 Cumorah Crest Drive Woodland Hills, CA 91364-3710

No. of
Copies Organization

1 Battelle Columbus Laboratories
ATTN: Mr. Victor Levin
505 King Ave.
Columbus, OH 43201-2693

1 Allegheny Ballistics Laboratory
Propulsion Technology Department
Hercules Aerospace Company
ATTN: Mr. Thomas F. Farabaugh
P.O. Box 210
Rocket Center, WV 26726

1 MBR Research Inc.
ATTN: Dr. Moshe Ben-Reuven
601 Ewing St., Suite C-22
Princeton, NJ 08540

Aberdeen Proving Ground

1 Cdr, CSTA
ATTN: STECS-PO, R. Hendricksen

USER EVALUATION SHEET/CHANGE OF ADDRESS

This laboratory undertakes a continuing effort to improve the quality of the reports it publishes. Your comments/answers below will aid us in our efforts.

1. Does this report satisfy a need? (Comment on purpose, related project, or other area of interest for which the report will be used.) _____

2. How, specifically, is the report being used? (Information source, design data, procedure, source of ideas, etc.) _____

3. Has the information in this report led to any quantitative savings as far as man-hours or dollars saved, operating costs avoided, or efficiencies achieved, etc? If so, please elaborate. _____

4. General Comments. What do you think should be changed to improve future reports? (Indicate changes to organization, technical content, format, etc.) _____

BRL Report Number BRL-TR-3275 Division Symbol _____

Check here if desire to be removed from distribution list. ____

Check here for address change. ____

Current address: Organization _____
Address _____

DEPARTMENT OF THE ARMY
Director
U.S. Army Ballistic Research Laboratory
ATTN: SLCBR-DD-T
Aberdeen Proving Ground, MD 21005-5066

OFFICIAL BUSINESS

BUSINESS REPLY MAIL
FIRST CLASS PERMIT No 0001, APG, MD

Postage will be paid by addressee

Director
U.S. Army Ballistic Research Laboratory
ATTN: SLCBR-DD-T
Aberdeen Proving Ground, MD 21005-5066

NO POSTAGE NECESSARY IF MAILED IN THE UNITED STATES